


RESEARCH PAPER



## Prediction and diversity of tracrRNAs from type II CRISPR-Cas systems

Te-yuan Chyou and Chris M Brown 

Department of Biochemistry, School of Biomedical Sciences, University of Otago, Dunedin, New Zealand

### ABSTRACT

Type II CRISPR-Cas9 systems require a small RNA called the trans-activating CRISPR RNA (tracrRNA) in order to function. The prediction of these non-coding RNAs in prokaryotic genomes is challenging because they have dissimilar structures, having short stems (3–6 bp) and non-canonical base-pairs e.g. G-A. Much of the tracrRNA is involved in base-pairing interactions with the CRISPR RNA, or itself, or in RNA-protein interactions with Cas9. Here we develop a new bioinformatic tool to predict tracrRNAs. On an experimentally verified test set the algorithm achieved a high sensitivity and specificity, and a low false discovery rate (FDR) on genome analysis. Analysis of representative RefSeq genomes (5462) detected 275 tracrRNAs from 165 genera. These tracrRNAs could be grouped into 15 clusters which were used to build covariance models. These clusters included *Streptococci* and *Staphylococci* tracrRNAs from the CRISPR-Cas9 systems which are currently used for gene editing. Compensating base changes observed in the models were consistent with the experimental structures of single guide RNAs (sgRNAs). Other clusters, for which there are not yet structures available, were predicted to form novel tracrRNA folds. These clusters included a large and divergent tracrRNA set from *Bacteroidetes*. These computational models contribute to the understanding of CRISPR-Cas biology, and will assist in the design of further engineered CRISPR-Cas9 systems. The tracrRNA prediction software is available through a galaxy web server.

### ARTICLE HISTORY

Received 26 February 2018  
Revised 2 July 2018  
Accepted 3 July 2018

### KEYWORDS

TracrRNA; CM model; small RNA; CRISPR-Cas

### Introduction

The CRISPR-Cas (Clustered Regularly Interspaced Palindromic Repeats, CRISPR-associated) system is an RNA mediated adaptive immune system. It is used by many bacterial and archaeal species to protect themselves from incoming foreign nucleic acids [1,2]. The simplest CRISPR-Cas systems consist of a CRISPR array and a set of CRISPR associated (Cas) proteins. The array encodes a non-coding RNA consisting of near identical ‘repeat’ sequences, with unique ‘spacer’ sequences between the repeats (Fig. 1). The spacers may be acquired from foreign nucleic acid sequences, notably viral DNA sequences. During subsequent viral infections, the CRISPR array will be transcribed as a non-coding RNA (precursor CRISPR RNA, pre-crRNA) and the Cas proteins expressed (Fig. 1). The pre-crRNA will then be processed into crRNA, which program the Cas proteins to target foreign nucleic acids. Specific Cas proteins or complexes then cleave the viral DNA.

There are multiple distinct types of CRISPR-Cas systems that are classified into two classes [3]. Class 1 types, namely type I and III CRISPR-Cas systems, consist of only Cas proteins and CRISPR arrays, and the pre-crRNAs can be processed directly into crRNAs.

Several Class 2 systems, notably type II A, B and C CRISPR-Cas systems also require a small non-coding RNA, the tracrRNA (trans-activating CRISPR RNA) in addition to Cas proteins and crRNAs (Fig. 1) [1,2,4,5]. These have been best studied in *Streptococcus pyogenes* (type II-A). In *S.*

*pyogenes* the tracrRNA is transcribed from two promoters into a precursor (pre-tracrRNA, 89 or 171 nt) that is processed into a mature tracrRNA of 75 nt [5]. In engineered systems this has been further shortened to a 67 nt synthetic tracrRNA [6].

The tracrRNAs have an ~ 25 nt ‘anti-repeat’, that is partly complementary to the CRISPR repeat sequence, followed by the ‘nexus’ [7], then a partially folded ‘tail’ [5,8] (Figs. 1 and 2). The pre-crRNAs will form a duplex with tracrRNAs by repeat-anti-repeat base-pairing, and then the RNAs are processed by the nuclease activity of Cas9 and RNase III (Fig. 1) [5,9,10]. After processing, the tracrRNA remains paired with the crRNA, interacting with the Cas9 protein through RNA-protein interactions. This facilitates the targeting and cleavage of target DNA [10], although some systems may also target RNA [11] (Fig. 1).

In addition to type II, the type V-B system (c2c1/cas12a) also includes a tracrRNA. However, the basepairing is at the 3’ rather than the 5’ end [12,13]. In this paper, we focus on type II tracrRNAs.

There have been relatively few studies of tracrRNAs in their natural bacterial systems, but considerable characterisation in heterologous systems. The type II system has been modified for use in genetic engineering by deleting much of the crRNA repeat-tracrRNA anti-repeat region and fusing the two RNAs into a single guide RNA (sgRNA) [8,14] or shortening in synthetic tracrRNA [6]. There has been a considerable amount of work done on the structure and functions of these sgRNAs in diverse organisms [1,15].



*S. pyogenes* (in the sgRNA) can eliminate cleavage activity completely, whereas the mutations tested in the other two stem-loops have no significant effect or only partially reduce activity [8,16]. In sgRNA constructs additional RNA loops or sequences have been added at the 3' end of the tracrRNA [21,22] or by extending SL2 of *S. pyogenes* gRNA [23,24] or SL2 of *S. aureus* gRNA [18] without impairing function.

In this study, we developed a tracrRNA predictor based on the elements of known tracrRNAs, and identified and analysed a large set of novel tracrRNA genes.

## Results

### Characteristics of known tracrRNAs

The anti-repeats of tracrRNAs have a partial complementarity to repeats in type II CRISPR-Cas9 systems, these repeats can be used for detection of anti-repeats in tracrRNAs. However, there are challenges in applying this matching on a genome-wide scale. Firstly small, partial, diverged, or degenerated arrays including repeats may be missed by stringent array prediction algorithms [25]. These repeats resemble anti-repeats on the reverse complement strand. Secondly, genomes may contain multiple types of arrays [26] e.g. arrays and repeats from type II and other types, but only the type II repeats will have corresponding anti-repeats in tracrRNAs. These first two challenges result in false positives. Thirdly, the repeat-anti-repeat matches may only have short regions of identity (< 10 nt). Fourthly, novel tracrRNAs may be dissimilar to known systems, due to divergence or possibly independent origins.

These last two challenges require flexible algorithms to avoid false negatives.

To develop a method for identifying tracrRNAs with high confidence, the features of a set of known tracrRNAs ( $n = 55$ ) were determined [4]. We then developed an automated system based on a support vector machine, that puts weights on these known features, but does not absolutely require them (Fig. 3).

We observed that these tracrRNAs are commonly located within 500 nt of *cas9*, although there are exceptions [4,16]. In addition, the crRNA repeat commonly starts with a GYY (G-pyrimidine-pyrimidine) and the tracrRNA tail commonly starts with AR (A-purine, Fig. 3, Fig. S1A-C).

Free energies for the formation of repeat-anti-repeat hybrids are typically below  $-40$  kcal/mol (Fig. S1D), however, there are frequently mismatches, including a bulge near the 5' end of the repeat (Fig. 2). The longest helices in the repeat-anti-repeat hybrids of known tracrRNAs are typically over 9 nt, and the proportion of non-pairing/mismatch nucleotides are typically below 20%. However, only one of the tracrRNAs has continuous pairing (34/36 nt, *Mycoplasma synoviae*). The data for all the known and predicted tracrRNAs are available in Supplement 3.

### Determining the parameters for the support vector machine (SVM)

A number of parameters were predicted from the training set, six were found to be most useful for the Support Vector Machine (SVM) classification. The 'length of the longest helix', and the 'proportion of non-pairing nucleotides' in the hybrid are used in the final SVM because they were good discriminators (triangles and circles in Fig. S2). In addition,

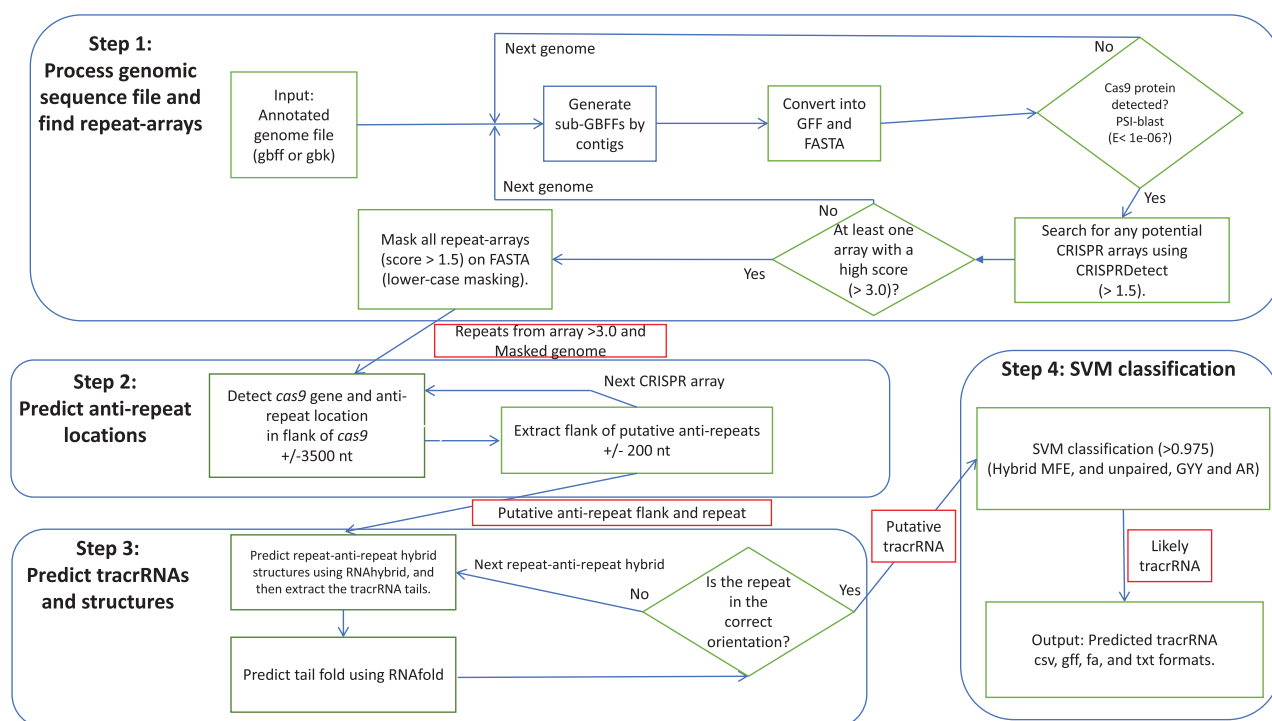


**Figure 3.** A flow diagram showing the process of tracrRNA prediction. (Results and Discussion and Methods). Step 1. Genomic files are processed to identify CRISPR arrays and *cas9* genes Step 2. Anti-repeats from putative tracrRNAs are detected and refined. Step 3. TracrRNA structures and features are predicted. Step 4. The putative tracrRNA are classified by an SVM, and predictions generated in multiple formats.

the minimum free energy of the hybrid, the *cas9*-tracrRNA intergenic distance, the presence of a 'GYY repeat-start' and the presence of an 'AR tail-start', were parameters used by the SVM (Fig. 3).

The SVM was tested by leave-one-out cross-validation using the positive and the negative training dataset, and the receiver operating characteristic (ROC) curve demonstrated the robustness of the SVM (Fig. S2). From the distribution of SVM true-positive probabilities of known tracrRNAs in the positive training dataset, the probability cutoff for true positives (TP) was chosen to be 0.975. One reported tracrRNA from *Legionella pneumophila* has a score lower than this (0.970), which may due to the presence of a 10 nt bulge on the anti-repeat side of the repeat-anti-repeat hybrid, that increases the proportion of non-pairing nucleotides.

### Genome wide prediction

- (1) We first identified genomes with both *cas9* genes and CRISPR arrays, by searching genomes for *cas9* genes using PSI-BLAST and Hidden Markov Models (HMMs), and CRISPR arrays were predicted using CRISPRDetect (Fig. 3). The CRISPR repeats from confidently predicted arrays (CRISPRDetect score > 3.0) were used to locate putative tracrRNA anti-repeats within 3500 bases of the *cas9* gene (see Methods). Annotated coding sequences and CRISPR arrays (score > 1.5) were not included in the search. In particular, imperfect arrays (scores 1.5–3.0) were excluded as they may have repeats that would generate false positives.

After locating the putative anti-repeats, the flank of the anti-repeat was extracted ( $\pm 200$ ). Repeat-anti-repeat hybrid structures and start position of the tracrRNA tails were predicted within this region using RNAhybrid [27], with constraints (Methods). The secondary structures of the tracrRNA tails were predicted using RNAfold [28]. The separate RNAhybrid (anti-repeat) and RNAfold (tail) predictions were combined. The direction of the anti-repeat depends on accurate prediction of the repeat direction. Therefore, we corrected the initial CRISPRDetect direction to increase accuracy for type II arrays (Methods), and eliminated matches from erroneous directions.

We used the prediction pipeline on all RefSeq 84 reference and representative bacterial genomes ( $n = 5462$ , Sept 2017) to predict tracrRNAs. We then selected all tracrRNA predictions with a single SVM TP probability of  $\geq 0.975$ . The dataset has 275 predicted tracrRNAs, including the 55 tracrRNAs in the SVM positive-training dataset from 165 genera (S3). The *Streptococcus pyogenes* M1 476 and the *Staphylococcus aureus* M0408 tracrRNAs was missed in this multi-genome screen, as both organisms are not representative bacterial species in RefSeq84 genomes. Our predictions also differ in lengths and start-end coordinates (Supplementary Figure S3). At the 5' end, we determined the likely end by using the repeat and locating the anti-repeat (using RNAhybrid). This will tend to give shorter predictions than the previous method that attempted to identify promoters. The median difference was 6 bases and interquartile range 2–16 bases (Supplementary Figure S2). In *C. jejuni*, our prediction

is 11 bases longer, extending the repeat-antirepeat base-pairing [4]. Such a longer precursor was reported by Dugar et al. 2013, although the major processed RNA detected was shorter [4,11,29]. Experimentally determined tracrRNAs are processed/shortened at the 5' end to within the repeat-antirepeat hybrid (Fig. 1).

At the 3' end compared to the previous analysis, the median difference was 3 bases and interquartile range 2–20 bases (Supplementary file S2). They predicted terminators using TransTermHP whereas we used a simpler method (TTTT) to estimate the end. For comparison we also used the best performing rho-independent terminator prediction software RNIE [30] to find rho-independent transcription terminators, but signals were only found in 17 of the 55 training-set tracrRNAs. These were all concordant with our predictions.

The characteristics of all the tracrRNA can be found in Supplementary file S4, their genomic contexts in S5, and mapping to a taxonomic tree in S6. In addition, there were 85 genomes with more than one tracrRNA prediction. It is possible that some genomes have more than one tracrRNA, but alternatively that the second prediction is a false positive. Our stringent SVM cutoff detects one or more tracrRNAs within 3500 bases in 360 of 482 *cas9* and CRISPR-array containing genomes. After excluding genomes with a truncated and potentially non-functioning *cas9* gene (< 2000 bases long), 299 out of 362 CRISPR have at least one tracrRNA, a sensitivity of 0.83. These 85 multiple predictions are provided in the supplements, but not used further for this initial conservative analysis. In the galaxy version of the tracrRNA predictor, *cas9* flanking distance, SVM cutoff, and other parameters can be varied by the user.

As an alternative measure of the FDR (false discovery rate), a region  $\pm 17,500$  bases flanking the *cas9* was examined, along with a range of SVM cutoffs (0.850 – 0.975). Most known tracrRNA lie within 3500 bases of the *cas9* (Fig S1), so additional predicted tracrRNAs in this longer sequence are likely false positives. At high stringency (0.975), after excluding genomes with a truncated *cas9* gene 302 genomes have at least one tracrRNA within 17,500 bases, of these there were 7 genomes with one or more potential 'false positive' tracrRNA predictions within 3,501–17,500 bases. This gives an FDR of 0.023 (7/302) at this cutoff. This data is shown in S5, and the best prediction within 3,500 bases for each gene in S3. A lower SVM cutoff of 0.95 gave an estimated FDR of 0.066 and sensitivity of 0.94 within 3500 nt of the *cas9* (Table S6). Such looser settings may be suitable for analysis of a few genomes of interest using the online tracrRNA predictor.

The direction of transcription of each of the three components of the type II systems were analysed. The most common arrangement of the three, found in 60% of those on a single contig, was that the *cas9* genes and tracrRNA were adjacent and transcribed in opposite directions followed by the CRISPR array (140/236 as sketched in Fig. 1). The CRISPR array was slightly more commonly (59%) transcribed in the same direction as the *cas* genes (83 vs 57) (Fig. 1).

### Clustering of tracrRNA sequences

We separately clustered the sequences of CRISPR repeats, anti-repeats, tracrRNA tails, and full length tracrRNAs of all

275 tracrRNAs. We further analysed those clusters with 3 or more sequences. Anti-repeats formed 19 clusters and tracrRNA tails formed 15 clusters. Repeats formed 23 clusters and full-length tracrRNAs formed 19 clusters. Cluster assignments, including two-member clusters, are shown on a taxonomic tree in S3. Sequences in clusters were aligned using CLUSTALW, and RNAalifold and covariance models built using CMbuild.

Clusters were compared, as covariance models, using CMcompare (Methods) to calculate the similarity between each pair of clusters, giving a 'link score'. A high link score indicates strong similarity. When the folds of the tail clusters were compared to themselves they had link scores 80–120, diagonal in Fig. 4A. In addition, some clusters generated similar models in addition what had been detected by the initial similarity (red boxes, notably 17 and 36, see below). However, in general, tails form distinct folds, with link scores below 40 (Fig. 4A).

Repeat and anti-repeat clusters correlate strongly (Chi-square = 1048.65, df 221, p-value < 1e-06, details not shown), as expected [5]. In addition, the relatively well conserved anti-repeat portion largely determines the tracrRNA cluster. Therefore, we further examined the most independent tracrRNA components – the anti-repeat and tail sequences and their common folds (Fig. 4B).

#### Association between anti-repeats and tracrRNA-tails

A possible path by which tracrRNAs evolved is from antisense transcription of the repeat [5]. In which case the initial tail would be any sequence following the anti-repeat. This could likely be a variable spacer sequence, or possibly a 3' trailer (Fig. 1). Depending on whether this happened once or independently in different clades, the sequences of tails and anti-repeats may, or may not, be associated.

We tested the correlation between anti-repeats and tracrRNA-tail members (Chi-square = 605.41, df 182, p-value < 1e-06, Fig. 4B). In most cases a single tracrRNA tail cluster correlates with an anti-repeat (AR) cluster, for example, tail cluster 1 and anti-repeat cluster 30, 9 and 36, 14 and 29 etc. In two cases anti-repeat clusters are split between two tail clusters. Particularly, tail cluster 15 is associated with AR clusters 11 and 33 and tail cluster 17 and 36 weakly associated with three AR clusters. This correlation supports the association between the repeat and the tracrRNA tail, rather than between tails across genera.

#### Common folds in tracrRNA sequences

We wanted to examine the similarities and differences between the folds in the tracrRNA tails. Fig. 6 shows the taxonomic relationship (NCBI) of the 165 representative genera that had tracrRNAs. Only those clades with tracrRNA tail clusters are shown in full (the full tree is in S5). For each genus, the assignments to tail clusters are shown, clades with no tracrRNA tail clusters are shown collapsed (Fig. 5). As noted in previous studies, tracrRNA tail sequences are highly diverse across species. In support of this diversity, those predicted in 124 of the 165 genera do not cluster. However,

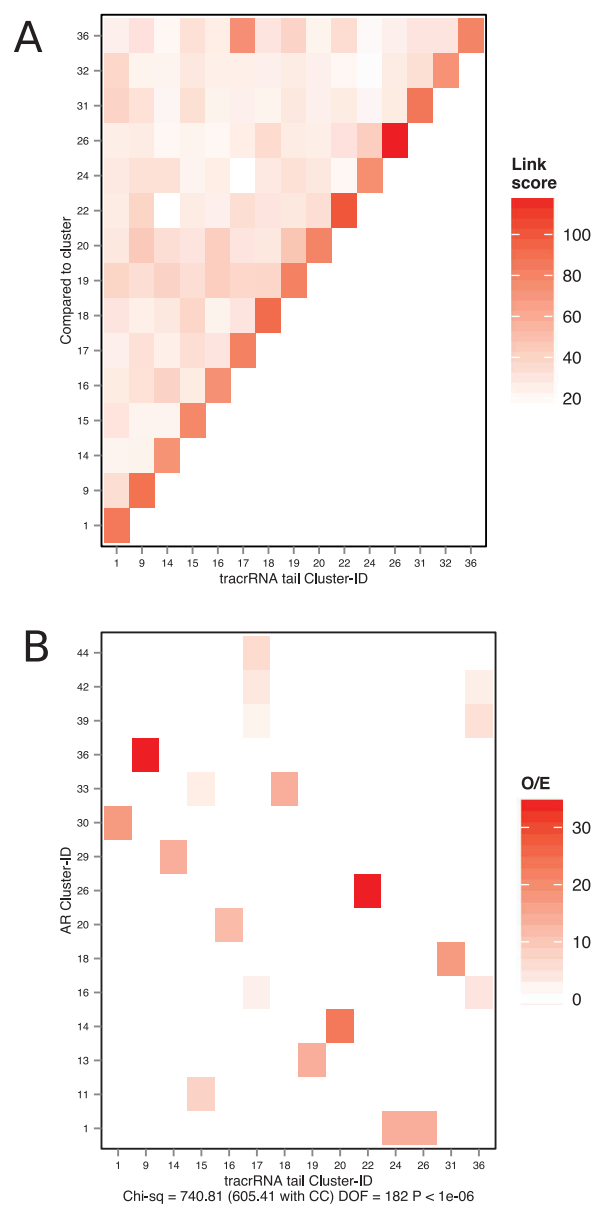


**Figure 4.** (A) Comparisons between tail-clusters. Similarities between clusters are calculated as link scores using CMCompare. A high link score indicates strong similarity (red). Self matches are on the diagonal. Only those clusters with 3 or more members were analysed so cluster IDs are discontinuous (e.g. 1, 9, 14). (B) the association between anti-repeats (AR) and tracrRNA tails. Most tail clusters correspond to one anti-repeat cluster (e.g. tail 1 and AR 30). To test for the association between anti-repeats and tracrRNA tails, we take tracrRNAs where the tail and the anti-repeat both belong to clusters with 3 or more sequences. The observed frequencies of tail and anti-repeat cluster assignments were divided by the expected frequencies of cluster assignments assuming that the tails and the anti-repeats are clustered independently.

where they do cluster it is notable that tracrRNA tails of related genera tend to fall within the same clusters (e.g. clusters 17, 19 and 36, Fig. 5.)

#### Streptococci tail clusters

The best characterised tracrRNA are those of *Streptococci*, particularly *S. pyogenes* and *S. thermophilus*, although much of their function has been inferred from studies done on gRNAs *in vitro* [8,31] or in heterologous environments (e.g.

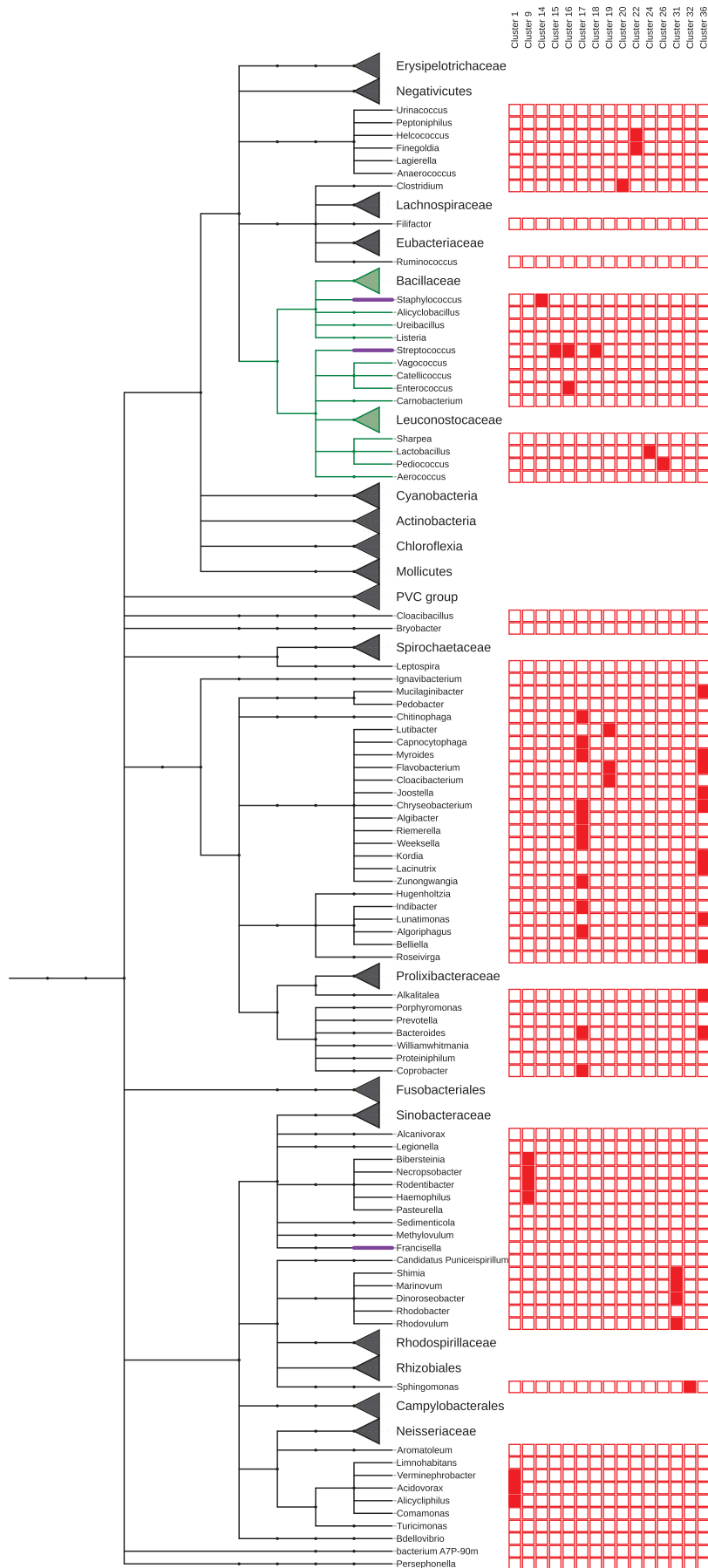


**Figure 5.** tracrRNA tail clusters distribution across genera. The relationships between the genera shown are based on NCBI's taxonomic database. Clades with no clusters are collapsed (triangles). Supplementary figure S3 is an extended version of this figure with 165 genera, tail, repeat, ant-repeat and tracrRNA clusters shown.







### Clustering of and evolution of tracrRNAs

It has previously been observed that the base-pairing patterns in repeat-anti-repeat hybrids are similar amongst closely related bacterial species [4,5]. We observed this in a much larger dataset. Furthermore, in this study, we observed a correlation between tracrRNA tails and the relationship between species. For each genus, the tracrRNAs tails tend to be located within the same cluster, or be split into clusters that are similar. It would be expected that *cas9* genes, tracrRNAs, and crRNAs co-evolve within species.

### Evolution of tracrRNAs

tracrRNA may have arisen from anti-sense transcription of repeats, then translocation of a repeat or proto-tracrRNA to a nearby part of the genome. Existing repeat sequences are diverse within CRISPR-Cas systems, reflecting likely multiple origins, but better conserved within type II systems. We cluster repeats into 23 clusters, including the three CRISPRMap type II repeat clusters [37]. It is possible that the tracrRNA may have evolved once, or multiple times, then co-evolved with CRISPR arrays and *cas9* genes. In order to begin to address this we looked for, and observed, association between the CRISPR anti-repeats and the tails of the corresponding tracrRNAs. CRISPR repeats of tracrRNAs from the same tail-sequence cluster tend to fall within specific repeat-sequence clusters, instead of spreading across all of them. This observation also supports co-evolution of repeat and tracrRNA. Regardless of whether the tracrRNA originated from a degenerated CRISPR array and/or the translocation of a degenerated CRISPR repeat, the tail of the tracrRNA co-evolves with the CRISPR array nearby.

### Genomic locations of tracrRNAs

We observed that the majority of tracrRNAs are transcribed from genes in the opposite direction to *cas9* but located nearby. The CRISPR arrays were commonly located after the *cas* genes in either orientation. This arrangement suggests possible co-regulation of the tracrRNAs and *cas9*, possibly being transcribed from a bidirectional promoter. On the other hand, the CRISPR array would have a separate promoter. If proto-tracrRNAs arose by antisense transcription of arrays then this may require subsequent translocation of the tracrRNA gene.

Most (45/55 training) tracrRNAs are located within 500 bases of the *cas9* gene. Notable exceptions are the Type II-C systems where some are adjacent and some have the *cas1* and *cas2* genes between the tracrRNA and *cas9*. This is similar to some of the II-A and II-B arrangements (e.g. *F. novicida* and *N. lactamica* c.f. *C. jejuni* [38]). This arrangement is only seen in *C. jejuni* in our analysis, not for example in the related *C. fetus* genome. This may indicate that the *C. jejuni* arrangement is exceptional.

### Other small CRISPR associated RNAs

Here, we have focussed on the tracrRNA of type II systems. Type V systems also have tracrRNAs, but they do not have a folded tail joining to the 3' end of the anti-repeat, instead, they

have a folded leader joining to the 5' end of the anti-repeat. Our predictor can, by design, detect the anti-repeat but did not extract the leader (data not shown). We propose to extend our predictor to extract tracrRNAs in Type V systems in the future. Furthermore, there is one other class of small RNAs that can also interact with CRISPRs. In the type II-B system of *Francisella novicida* there is an additional unique small CRISPR/Cas-associated RNA (scaRNA) [39,40]. This RNA, and the tracrRNA have an additional role: to repress an endogenous bacterial lipoprotein (*blp*) mRNA [39,41,42]. In this process the 5' end of the tracrRNA (anti-repeat) base-pairs to the mRNA, rather than crRNA [39–42]. In our analysis this scaRNA overlaps the CRISPR array and is masked.

The CRISPR-Cas system has been modified for genetic engineering, and the role of tracrRNA/gRNA is to facilitate site-specific gene modification at high precision. In addition to the understanding of CRISPR-Cas biology, these computational models of tracrRNAs will assist in the design of engineered CRISPR-Cas9 systems.

## Materials and methods

### Training datasets for the SVM

From published tracrRNA [4] we built the positive training dataset, adding the tracrRNA of *S. aureus*, giving a total of 55 tracrRNAs. Precise ends of 10 of the 55 tracrRNAs have been confirmed experimentally. Our SVM classifier was trained based on the attributes of the repeat-anti-repeat hybrid and the 3-way junction parts of the repeat-tracrRNA duplex, as well as the distance between the tracrRNA and the *cas9* gene. Attributes of the tracrRNA tail were not considered in the prediction, to allow unbiased tracrRNA-tail sequence analyses.

To build the positive training dataset, genomic sequence files in GBFF format were downloaded from RefSeq 84. For each published tracrRNA, we reproduced it by using CRISPRDetect to generate the CRISPR array at an array-quality score cutoff of 3.0, BLASTN to locate the anti-repeat (word-size 7, mismatch penalty -1, gap-opening penalty -2, gap-extension penalty -1, match-reward 1, and e-value cutoff 20), and RNAhybrid to calculate the repeat-anti-repeat hybrid structure and locate the 3-way junction.

The CRISPR repeat sequence was then used as a query to find the anti-repeat part of the tracrRNA in the BLASTN step. Genomic sequence was then extracted around the anti-repeat. We then applied RNAhybrid to the CRISPR repeat and the extracted genomic sequence with default settings but requiring at least one base-pair from position 1 to 3 relative to the 5' end of the repeat, to calculate the repeat-anti-repeat hybrid structure and the free-energy, and at the same time locate the end of the hybrid. We then extracted the tail of the tracrRNA up to the next U-tetramer, U tetramers were not considered in the first 40 nucleotides.

Because the prediction of repeat direction is not completely accurate [25] we tested both orientations. The initial prediction of the direction of the array was done using CRISPRDetect, and for type II arrays, the direction prediction was further refined based on features of known type-II arrays and tracrRNAs.

Type II CRISPR repeats commonly begin with GYY and this was used as the primary indicator of direction. If both, or none of, the array repeat predictions began with GYY repeat start, we used the CRISPRDetect/CRISPRDirection prediction. All tracrRNAs with a tail starting with the conserved AR, were retained as an alternative (Fig. S4). This algorithm will not eliminate potential tracrRNAs where the CRISPR repeats differ and do not start with GYY or the tails do not start with AR.

After the direction-reconfirmation step, for each tracrRNA prediction we calculated the probability of a true-positive prediction with a support-vector machine (SVM). The SVM has 6 parameters. The presence of the conserved GYY repeat start, and the presence of the conserved AR tail start supported the CRISPR array direction chosen as well as building the SVM. The minimum free-energy (MFE) of the repeat-anti-repeat hybrid, the tracrRNA-Cas9 intergenic distance, the length of the longest helix in the repeat-anti-repeat hybrid, and the proportion of non-pairing nucleotides in the repeat-anti-repeat hybrid, were also included in the SVM.

Additional statistical parameters, such as position of the first bulge in the repeat-anti-repeat hybrid from the three-way junction and the nucleotide composition of the repeat-anti-repeat hybrid, were also considered, but including them in the SVM did not increase prediction accuracy (not shown).

To build negative training dataset, for each CRISPR repeat we randomly shuffled the CRISPR repeat and the corresponding tracrRNA to generate a 'false CRISPR repeat' and a 'false tracrRNA'. These were matched using RNA-hybrid, if a hybrid is not found after shuffling the sequences, the randomisation process was repeated until a hybrid was detected. A randomly selected intergenic distance was assigned assuming that the false tracrRNA can be anywhere in the genome but not within the *cas9* gene.

Specific parameters of the SVM were chosen after extracting and analysing the positive and the negative training datasets. In general terms, the characteristics that published tracrRNAs had in common, or are discriminators of true tracrRNAs, were considered as potential SVM parameters. The final SVM was built using the application SVM-train in the LIBSVM suite [43]. We used the two-class support-vector classifier with radial-basis kernel function under the default settings. The SVM was validated by leave-one-out cross-validation using the positive and negative training datasets. The robustness of the SVM was evaluated by plotting and examining the ROC curve.

### Genome wide predictions of tracrRNAs

Amino acid sequences in the GBFF files are extracted. PSI-Blast was then used with an e-value cutoff of 1e-06 to search for Cas9 using the multiple-alignments of Cas9-family proteins published by Makarova et al 2015 [44] (PSI-BLAST models mkCas0193, cd09643, COG3513, cd09704 and mkCas0192), and the start-end coordinates of the Cas9 coding sequence were determined. This process was complemented by a hidden Markov model search using HMMsearch with an e-value cutoff of 1e-06, using HMM models of Cas9 published by Burstein et al 2016 [45].

In a similar way to the construction of the positive training dataset, for each genome with a Cas9 prediction, we used

CRISPRDetect to predict putative CRISPR arrays (array-quality score cutoff 3.0). Then we masked out all annotated genes and all CRISPR-arrays predicted, and used BLASTN to locate the anti-repeat parts of putative tracrRNAs using the same set of parameters we used to generate the positive training dataset, and the CRISPR repeat sequences as queries. We then extracted genomic flanking sequences around the putative anti-repeats, and applied RNAhybrid to the CRISPR repeats predicted and the genomic extracts, to calculate the repeat-anti-repeat hybrid structures and the free energies, and at the same time locate the 3-way junctions of the repeat-tracrRNA duplexes. RNAhybrid were run using the following constraints: base-pairing in the first three positions of the repeat-anti-repeat hybrid, 3–15 mismatches in the hybrid, and a helix of over 9 base-pairs. RNAhybrid allows such constraints as has been used for the similar task of determining miRNA-mRNA interactions[46]. The region following the anti-repeat (the tracrRNA tail) was extracted, minimum length 40, max 204 up to the first four U's (a putative terminator). The structure of the repeat-tracrRNA duplex were also calculated using RNAcofold [47] and examined using regular expressions corresponding to known tracrRNA families (shown in S3). The secondary structure of the tracrRNA tails were predicted using RNAfold. RNAfold and RNAcofold were run with default settings, but without allowing for lonely base-pairs.

Because the prediction of array direction or strand was not always congruent with published data, both the predicted CRISPR repeat and the reverse-complement of it were used to predict tracrRNAs. We examined repeat-anti-repeat hybrids of known tracrRNAs to find conserved sequences in the CRISPR repeat (GYY) and the 3-way junction part of the tracrRNAs (AR), and used them to re-determine the array direction.

The SVM was applied to all tracrRNA predictions, to calculate the probability of a TP prediction. This calculation was accomplished by using the application SVM-predict in the LIBSVM suite. To establish a probability cutoff for true predictions, we applied the established prediction pipeline including the SVM to re-predict the known tracrRNAs in the positive training dataset to calculate the TP probabilities and examined their distribution.

### Software availability

- (2) The software is available through a galaxy server (galaxy.otago.ac.nz). Data is available as supplements, and updates will be available from <http://bioanalysis.otago.ac.nz/tracrRNA>.

### Mapping tracrRNA positions back to genomes

The positions of the *cas9* (HMM search on RefSeq predicted proteins, methods above), CRISPR arrays (CRISPRDetect), and tracrRNAs were recorded (csv table in S4). This was used to determine the order and orientation of these genes. The flanking regions of the tracrRNAs (+/- 5000 nt) were extracted and re-annotated using an in house modified version of prokka [48]. The genbank format output (.gbk) was visualised in Geneious [49] (S5).

## Clustering of *tracrRNA* sequences

Clustering of repeats, anti-repeats, *tracrRNAs* and tails was done using UCLUST [50] at an identity cutoff of 0.65. Alignments were made of the sequences in each cluster [51]. We then made covariance models from the tail cluster alignments using CMbuild [52] using default parameters, and compared them using CMcompare [53]. Consensus fold of each tail-cluster alignment were calculated using RNAAlifold [54], and visualized them using Ralee [55]. Alignments, Stockholm format files, and covariance models are available in S4. Repeats for all CRISPR types have been clustered previously as part of CRISPRMap [37], co-occurrence between the three type II clusters and those generated here is shown in S4.

## Comparison of common folds in clusters

Comparisons were made using CMcompare [52]. To determine to significance of the co-clustering of anti-repeats and *tracrRNA* tails, we selected *tracrRNAs* where the anti-repeat and tail belong to clusters of 3 or more sequences. The observed frequencies (O) of tail and anti-repeat cluster assignments, and the expected frequencies (E) of tail and anti-repeat cluster assignments assuming statistical independence, were calculated; and the O/E values were visualized on a heatmap in R. A Chi-Squared test was used to test the significance of co-clustering.

## Disclosure of Potential Conflicts of Interest

No potential conflict of interest was reported by the authors.

## Funding

This work was supported by the Marsden Fund Council from Government funding, managed by Royal Society Te Apārangi, and a University of Otago Grant.

## ORCID

Chris M Brown  <http://orcid.org/0000-0001-6986-5342>

## References

- Jiang F, Doudna JA. CRISPR-Cas9 structures and mechanisms. *Annu Rev Biophys.* 2017;46:505–529.
- Mir A, Edraki A, Lee J, et al. Type II-C CRISPR-Cas9 biology, mechanism, and application. *ACS Chem Biol.* 2018;13:357–365.
- Koonin EV, Makarova KS, Zhang F. Diversity, classification and evolution of CRISPR-Cas systems. *Curr Opin Microbiol.* 2017;37:67–78.
- Chylinski K, Le Rhun A, Charpentier E. The *tracrRNA* and Cas9 families of type II CRISPR-Cas immunity systems. *RNA Biol.* 2013;10:726–737.
- Deltcheva E, Chylinski K, Sharma CM, et al. CRISPR RNA maturation by trans-encoded small RNA and host factor RNase III. *Nature.* 2011;471:602–607.
- Jacobi AM, Rettig GR, Turk R, et al. Simplified CRISPR tools for efficient genome editing and streamlined protocols for their delivery into mammalian cells and mouse zygotes. *Methods.* 2017;121–122:16–28.
- Briner AE, Donohoue PD, Gomaa AA, et al. Guide RNA functional modules direct Cas9 activity and orthogonality. *Mol Cell.* 2014;56:333–339.
- Nishimasu H, Ran FA, Hsu PD, et al. Crystal structure of Cas9 in complex with guide RNA and target DNA. *Cell.* 2014;156:935–949.
- Carte J, Christopher RT, Smith JT, et al. The three major types of CRISPR-Cas systems function independently in CRISPR RNA biogenesis in *Streptococcus thermophilus*. *Mol Microbiol.* 2014;93:98–112.
- Charpentier E, Richter H, van der Oost J, et al. Biogenesis pathways of RNA guides in archaeal and bacterial CRISPR-Cas adaptive immunity. *FEMS Microbiol Rev.* 2015;39:428–441.
- Dugar G, Leenay RT, Eisenbart SK, et al. CRISPR RNA-Dependent Binding and Cleavage of Endogenous RNAs by the *Campylobacter jejuni* Cas9. *Mol Cell.* 2018;69:893–905 e7.
- Shmakov S, Smargon A, Scott D, et al. Diversity and evolution of class 2 CRISPR-Cas systems. *Nat Rev Microbiol.* 2017;15:169–182.
- Shmakov S, Abudayyeh OO, Makarova KS, et al. Discovery and functional characterization of diverse class 2 CRISPR-Cas systems. *Mol Cell.* 2015;60:385–397.
- Jinek M, Chylinski K, Fonfara I, et al. A programmable dual-RNA-guided DNA endonuclease in adaptive bacterial immunity. *Science.* 2012;337:816–821.
- Yamada M, Watanabe Y, Gootenberg JS, et al. Crystal structure of the minimal Cas9 from *Campylobacter jejuni* reveals the molecular diversity in the CRISPR-Cas9 systems. *Mol Cell.* 2017;65:1109–1121.
- Briner AE, Henriksen ED, Barrangou R. Prediction and validation of native and engineered Cas9 guide sequences. *Cold Spring Harb Protoc.* 2016;2016:pbprot086785.
- Briner AE, Lugli GA, Milani C, et al. Occurrence and diversity of CRISPR-Cas systems in the genus *Bifidobacterium*. *PLoS One.* 2015;10:e0133661.
- Nishimasu H, Cong L, Yan WX, et al. Crystal structure of *Staphylococcus aureus* Cas9. *Cell.* 2015;162:1113–1126.
- Hirano H, Gootenberg JS, Horii T, et al. Structure and engineering of *Francisella novicida* Cas9. *Cell.* 2016;164:950–961.
- Swarts DC, van der Oost J, Jinek M. Structural basis for guide RNA processing and seed-dependent DNA targeting by CRISPR-Cas12a. *Mol Cell.* 2017;66:221–233 e4.
- Mali P, Aach J, Stranges PB, et al. CAS9 transcriptional activators for target specificity screening and paired nickases for cooperative genome engineering. *Nat Biotechnol.* 2013;31:833–838.
- Cheng AW, Jillette N, Lee P, et al. Casilio: a versatile CRISPR-Cas9-Pumilio hybrid for gene regulation and genomic labeling. *Cell Res.* 2016;26:254–257.
- Konermann S, Brigham MD, Trevino AE, et al. Genome-scale transcriptional activation by an engineered CRISPR-Cas9 complex. *Nature.* 2015;517:583–588.
- Zalatan JG, Lee ME, Almeida R, et al. Engineering complex synthetic transcriptional programs with CRISPR RNA scaffolds. *Cell.* 2015;160:339–350.
- Biswas A, Staals RH, Morales SE, et al. CRISPRDetect: a flexible algorithm to define CRISPR arrays. *BMC Genomics.* 2016;17:356.
- Shmakov SA, Sitnik V, Makarova KS, et al. The CRISPR spacer space is dominated by sequences from species-specific mobilomes. *MBio.* 2017;8:e01397–17.
- Kruger J, Rehmsmeier M. RNAhybrid: microRNA target prediction easy, fast and flexible. *Nucleic Acids Res.* 2006;34:W451–W454.
- Hofacker IL, Fontana W, Stadler PF, et al. Fast folding and comparison of RNA secondary structures. *Monatsh Chem.* 1994;125:167–188.
- Dugar G, Herbig A, Forstner KU, et al. High-resolution transcriptome maps reveal strain-specific regulatory features of multiple *Campylobacter jejuni* isolates. *PLoS Genet.* 2013;9:e1003495.
- Gardner PP, Barquist L, Bateman A, et al. RNIE: genome-wide prediction of bacterial intrinsic terminators. *Nucleic Acids Res.* 2011;39:5845–5852.

31. Karvelis T, Gasiunas G, Miksys A, et al. crRNA and tracrRNA guide Cas9-mediated DNA interference in *Streptococcus thermophilus*. *RNA Biol.* **2013**;10:841–851.
32. Nishimasu H, Yamano T, Gao L, et al. Structural Basis for the Altered PAM Recognition by Engineered CRISPR-Cpf1. *Mol Cell.* **2017**;67:139–147 e2.
33. Najm FJ, Strand C, Donovan KF, et al. Orthologous CRISPR-Cas9 enzymes for combinatorial genetic screens. *Nat Biotechnol.* **2017**;36:179–189.
34. Ran FA, Cong L, Yan WX, et al. In vivo genome editing using *Staphylococcus aureus* Cas9. *Nature.* **2015**;520:186–191.
35. Tajkarimi M, Hm W. CRISPR-Cas systems in bacteroides fragilis, an important pathobiont in the human gut microbiome. *Front Microbiol.* **2017**;8:2234.
36. Zhu DK, Yang XQ, He Y, et al. Comparative genomic analysis identifies structural features of CRISPR-Cas systems in *Riemerella anatipestifer*. *BMC Genomics.* **2016**;17:689.
37. Alkhnbashi OS, Costa F, Shah SA, et al. CRISPRstrand: predicting repeat orientations to determine the crRNA-encoding strand at CRISPR loci. *Bioinformatics.* **2014**;30:489–496.
38. Pearson BM, Louwen R, van Baarlen P, et al. Differential distribution of type II CRISPR-Cas systems in agricultural and nonagricultural *Campylobacter coli* and *Campylobacter jejuni* isolates correlates with lack of shared environments. *Genome Biol Evol.* **2015**;7:2663–2679.
39. Sampson TR, Weiss DS. Cas9-dependent endogenous gene regulation is required for bacterial virulence. *Biochem Soc Trans.* **2013**;41:1407–1411.
40. Sampson TR, Saroj SD, Llewellyn AC, et al. A CRISPR/Cas system mediates bacterial innate immune evasion and virulence. *Nature.* **2013**;497:254–257.
41. Westra ER, Buckling A, Fineran PC. CRISPR-Cas systems: beyond adaptive immunity. *Nat Rev Microbiol.* **2014**;12:317–326.
42. Hille F, Richter H, Wong SP, et al. The Biology of CRISPR-Cas: backward and Forward. *Cell.* **2018**;172:1239–1259.
43. Chang CC, Lin C-J. LIBSVM: a library for support vector machines. *ACM Trans Intell Syst Technol.* **2011**;2:1–27.
44. Makarova KS, Wolf YI, Alkhnbashi OS, et al. An updated evolutionary classification of CRISPR-Cas systems. *Nat Rev Microbiol.* **2015**;13:722–736.
45. Burstein D, Harrington LB, Strutt SC, et al. New CRISPR-Cas systems from uncultivated microbes. *Nature.* **2017**;542:237–241.
46. Umu SU, Gardner PP. A comprehensive benchmark of RNA-RNA interaction prediction tools for all domains of life. *Bioinformatics.* **2017**;33:988–996.
47. Bernhart SH, Tafer H, Muckstein U, et al. Partition function and base pairing probabilities of RNA heterodimers. *Algorithms Mol Biol.* **2006**;1:3.
48. Seemann T. Prokka: rapid prokaryotic genome annotation. *Bioinformatics.* **2014**;30:2068–2069.
49. Kearse M, Moir R, Wilson A, et al. Geneious basic: an integrated and extendable desktop software platform for the organization and analysis of sequence data. *Bioinformatics.* **2012**;28:1647–1649.
50. Edgar RC. Search and clustering orders of magnitude faster than BLAST. *Bioinformatics.* **2010**;26:2460–2461.
51. Larkin MA, Blackshields G, Brown NP, et al. Clustal W and Clustal X version 2.0. *Bioinformatics.* **2007**;23:2947–2948.
52. Nawrocki EP, Eddy SR. Infernal 1.1: 100-fold faster RNA homology searches. *Bioinformatics.* **2013**;29:2933–2935.
53. Honer Zu Siederdisen C, Hofacker IL. Discriminatory power of RNA family models. *Bioinformatics.* **2010**;26:453–459.
54. Bernhart SH, Hofacker IL, Will S, et al. RNAalifold: improved consensus structure prediction for RNA alignments. *BMC Bioinformatics.* **2008**;9:474.
55. Griffiths-Jones S. RALEE-RNA ALignment editor in Emacs. *Bioinformatics.* **2005**;21:257–259.
56. Garcia-Doval C, Jinek M. Molecular architectures and mechanisms of Class 2 CRISPR-associated nucleases. *Curr Opin Struct Biol.* **2017**;47:157–166.